

MODULAR JET AND PROPELLER ENGINE – PART I: INITIAL STUDIES

Tom Otten[1], Tomasz Matuschek[1], Jannik Häßy[1], Julie Frank[2] & Robin G. Brakmann[2]

[1]German Aerospace Center (DLR), Institute of Propulsion Technology, Engine department
[2]German Aerospace Center (DLR), Institute of Propulsion Technology, Turbine department

Abstract

Small unmanned aerial vehicles increasingly require propulsion systems that combine high thrust-to-weight ratio with improved fuel efficiency at low and medium flight speeds. This paper investigates a modular retrofit concept in which a small off-the-shelf turbojet engine is operated as a fixed gas generator and extended by an additional power turbine and propeller. The concept, termed Modular Jet and Propeller Engine (MOJO), aims to increase propulsive efficiency without major modifications to the baseline turbojet.

Two configurations are investigated: a geared layout, in which turbine and propeller speeds are decoupled by a reduction gearbox, and a direct-drive layout, in which both components operate at the same rotational speed. For both configurations, preliminary turbine and propeller designs are generated using conceptual design methods and integrated into an engine performance model.

The results show that both propeller-based retrofit configurations can substantially reduce thrust-specific fuel consumption compared with the baseline turbojet by increasing the useful thrust through improved propulsive efficiency. The geared configuration provides a more robust performance solution, at the cost of potentially higher volume and mass linked to the additional gearbox components. The direct-drive configuration eliminates the gearbox but is constrained by the common turbine-propeller speed, resulting in high blade-tip Mach numbers and reduced propeller efficiency.

Keywords: Propulsion, Turbojet, Turboprop, Conceptual Design

1. Introduction

The use of unmanned aerial vehicles (UAVs) has gained importance in recent years in both civil and military applications. This trend is expected to intensify further in the foreseeable future. A wide range of UAV configurations and mission profiles is currently being developed, resulting in a substantial demand for a variety of propulsion systems capable of covering a broad spectrum of performance requirements.

UAVs designed for high flight speeds (exceeding Mach 0.6) are predominantly equipped with small turbojet engines. Their favorable high thrust-to-weight ratio and their high specific thrust allow efficient thrust generation at high flight speeds. However, the high jet exit velocity of turbojets results in poor propulsive efficiency at lower flight speeds.

In contrast, propeller-based propulsion systems provide substantially higher propulsive efficiency in low- and medium-speed flight regimes. Electric-motor- or piston-engine-driven propellers are commonly used for small UAVs, while turboprop engines become attractive for larger vehicles and increasing thrust or range requirements. The achievable maximum flight speed of propeller-driven aircraft is limited by decreasing propeller efficiency at higher subsonic Mach numbers.

In the past, developments in civil and military aircraft engines have often built upon each other. Previously developed core engines are frequently used as the basis for new propulsion systems, either in unchanged form, in a scaled configuration, or with limited modifications to selected blade rows. This common-core approach reduces development time, risk, and cost, while also enabling manufacturing economies of scale [1], [2].

Given the diverse development paths currently emerging in the field of small-scale propulsion systems, the transfer of this strategy to small-scale turbo engines is becoming increasingly attractive. Small-scale turbo engines are comparatively simple in architecture and often consist of only one

compressor stage and one turbine stage; therefore, complex common-core strategies are not directly applicable. However, by extending a conventional small turbojet with an additional power turbine and a propeller, the jet engine can be operated as a gas generator for a turboprop configuration—an approach referred to as a common gas generator. This concept can be implemented such that the added power turbine and propeller form a modular unit that can be attached to an existing turbojet engine without significant structural modifications of the turbojet (retrofit). This modular concept is referred to as the Modular Jet and Propeller Engine (MOJO) and constitutes the main focus of the work presented in this paper.

The objective of this paper is to present and evaluate possible approaches for implementing such a MOJO retrofit kit. This is done by comparing conventional combinations of the power turbine connected to the propeller via a reduction gearbox with a directly coupled approach. Furthermore, the operational behavior of a turbojet engine with and without the retrofit kit is analyzed and compared.

2. Concept and modeling approach

Improving the propulsive efficiency of small turbojet engines at lower flight speeds is not trivial. The implementation of conventional turbofan architectures is generally impractical for very small engines, as their simple single-stage compressor configuration provides limited capability for integrating an efficient bypass system.

Alternative concepts include ejector nozzles, which reduce specific thrust by entraining additional airflow into the exhaust jet. However, the achievable efficiency improvements are limited [3].

A more effective solution for low- and medium-speed applications is the integration of a propeller. This substantially increases propulsive efficiency but limits the achievable maximum flight speed due to propeller compressibility and tip speed constraints. The transfer of power from the gas turbine core to the propeller can be realized in several ways. In principle, mechanical power may be extracted directly from an existing shaft within the engine. However, this approach is typically constrained, as it alters the operating points of both the compressor and turbine, thereby affecting overall engine performance and stability.

In most practical implementations, power is extracted from the exhaust flow downstream of the high-pressure turbine by introducing an additional turbine stage, commonly referred to as a free power turbine. Owing to the substantially different rotational speed requirements of the propeller compared to the core engine, this turbine is usually mounted on a separate shaft.

In modern large turboprop and turboshaft configurations, the mechanical power generated by the free turbine is typically transmitted forward through the engine to drive a front-mounted propeller. A pusher configuration with a rear-mounted propeller is also feasible. This arrangement can be advantageous when modifications to an existing core engine are to be minimized, as it avoids the need to route an additional shaft through the engine. However, positioning the propeller downstream of the hot section of the core engine introduces thermal challenges.

Power transmission between the free turbine and the propeller is conventionally achieved via a mechanical shaft and reduction gearbox to decouple the rotational speeds of the turbine and the propeller. Configurations without a gearbox are referred to as direct-drive configurations and require the turbine and propeller to operate at the same rotational speed. As an alternative, the mechanical power can be converted into electrical energy using a generator coupled to the turbine shaft, with the propeller subsequently driven by an electric motor.

2.1 Baseline turbojet model

In the present study, a generic turbojet engine with a sea-level static (SLS) thrust of 1000 N is selected as the reference use case. The detailed design of the turbojet itself is not the primary focus of this study, since the engine serves as a replaceable baseline configuration. The objective of the engine model is therefore to provide a representative baseline of current small turbojet technology for the subsequent power turbine analysis. The thermodynamic cycle parameters and design characteristics of the baseline model are selected to represent the performance of typical small turbojet engines using publicly available manufacturer data. Particular attention is given to realistic turbine exit temperatures and fuel consumption, as these quantities are often published by engine

manufacturers, e.g. [4].

Most engines in this thrust class follow a similar architecture. They typically consist of a radial compressor and an uncooled turbine mounted on a common shaft, with a combustor using vaporizer tubes located between the compressor and the turbine. The shaft bearings are usually equipped with a total-loss lubrication system that uses jet fuel mixed with turbine oil. The propulsive thrust is generated by a convergent nozzle. The thermodynamic schematic of the baseline model is shown in Figure 1.

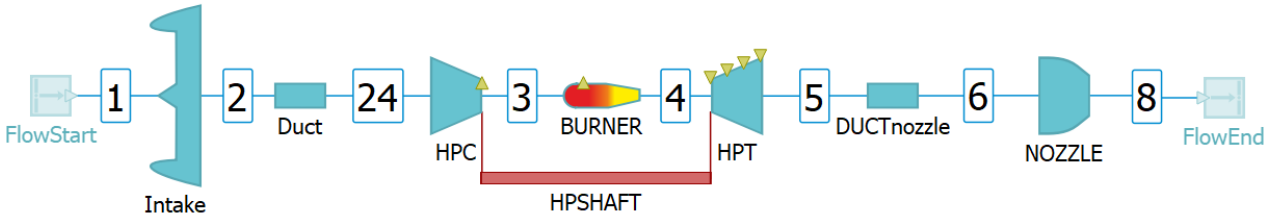


Figure 1 – Baseline engine thermodynamic schematic

The main design assumptions are summarized in Table *1*. For the compressor pressure ratio, a value of 4.3 is assumed. Representative efficiencies are applied for both the compressor and the turbine. The combustion efficiency is assumed to be comparatively low, particularly at part load. The total-loss lubrication system further reduces the effective fuel efficiency, since part of the supplied fuel is used for lubrication and not for combustion.

As the turbine is uncooled, the turbine inlet temperature is limited by the material properties. Assuming Inconel as the material for the uncooled turbine, a limit for the turbine entry temperature of 1150 K is set. For the Exhaust Gas Temperature (EGT) a value of 720 K is targeted.

Typical pressure losses are assumed in the intake to take into account the aerodynamic losses of the SMG (Starter Motor Generator) that is typically integrated here.

Name	Value
Compressor Pressure Ratio	4.3
Turbine Entry Temperature	1150 K
Exhaust gas temperature	720 K
Mass flow	1.84 kg/s
Compressor design efficiency	79 %
Turbine design efficiency	85 %
Combustion design efficiency (including losses for lubrication)	85 %
Resulting Thrust @ SLS	1000 N
Resulting TSFC @ SLS	39 g/kNs

Table 1 – Main performance values for the baseline engine at sea-level-static

2.2 Modeling approach for the MOJO configurations

The gas generator is assumed to be fixed. Therefore, the jet-engine cycle parameters are kept unchanged. To avoid any geometric modification of this core engine, a pusher configuration is assumed for the propeller, as it is the only arrangement compatible with this constraint. A puller configuration would require a propeller shaft to pass through the gas generator, resulting in major modifications to the existing components.

A free power turbine (PT) is introduced downstream of the high-pressure turbine (HPT) to extract mechanical power from the exhaust flow. A nozzle is placed downstream of the power turbine and sized such that, under nominal operating conditions, the operating condition of the gas generator remains unaffected by the power turbine.

The theoretical maximum power $P_{max,theoretical}$ that can be extracted from the flow downstream of

the gas generator can be estimated by:

$$P_{max,theoretical} = \dot{m} * c_p * T_{45} * \left(1 - \left(\frac{p_{45}}{p_{amb}}\right)^{-\frac{\kappa-1}{\kappa}}\right) \quad (1)$$

In which $\dot{m}$ is the mass flow, T_{45} and p_{45} are the total temperature and pressure at the inlet of the power turbine, κ is the isentropic exponent and c_p is the heat capacity of the flow.

This expression represents an ideal limit and does not account for losses in the power turbine, shaft, gearbox, or propeller. Consequently, the practically achievable shaft power is lower than the theoretical maximum. In addition, to avoid infeasible large nozzle geometries, a minimum nozzle pressure ratio must be maintained, which further limits the extractable power.

Figure 2 illustrates the effect of power extraction on the resulting nozzle pressure ratio for different turbine efficiencies, while neglecting other losses.

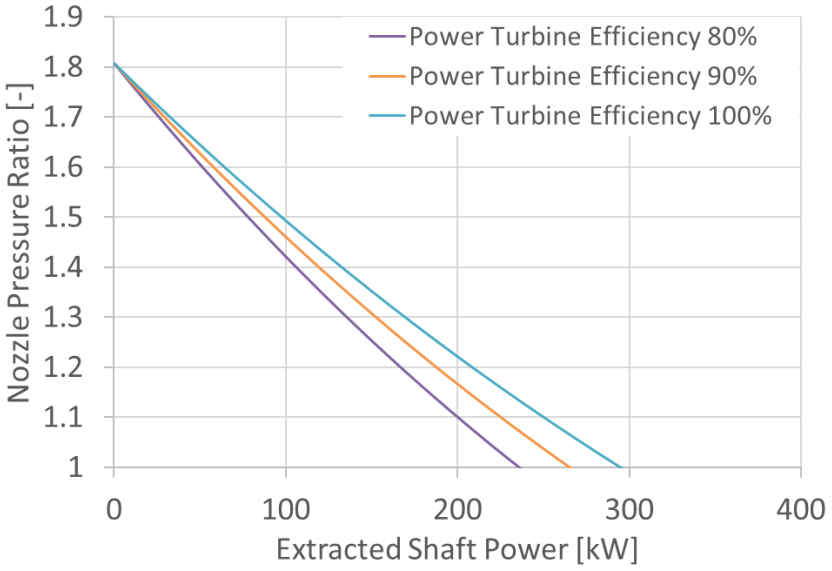


Figure 2 – Influence of power extraction on nozzle pressure ratio at SLS

Assuming a minimum remaining nozzle pressure ratio of 1.01 at SLS and at maximum rotational speed, for an isentropic turbine efficiency of 80 % approximately 240 kW of shaft power can be extracted from the exhaust flow of the gas generator.

Regarding the transmission of this power to the propeller, multiple configurations are considered. The conventional approach employs a reduction gearbox between the power turbine and the propeller allowing both components to operate at their respective optimal rotational speeds at the design point. As an alternative, a direct-drive configuration is analyzed, in which the power turbine and propeller operate at the same rotational speed.

For the propeller design, an initial flight Mach number of 0.4 is assumed. Consequently, the subsequent propeller and power turbine designs are not performed for SLS conditions, but for this flight Mach number.

3. Geared MOJO configuration

In the geared retrofit configuration, a gearbox is used to decouple the rotational speed of the power turbine from the rotational speed of the propeller. This allows the power turbine to be designed at a comparatively high rotational speed, while the propeller can be operated at a lower speed in order to limit blade tip Mach number and maintain propeller efficiency.

A schematic concept illustration of this configuration is shown in Figure 3. The illustration is intended to clarify the overall engine architecture and component arrangement; it is not based on the calculated component geometries.

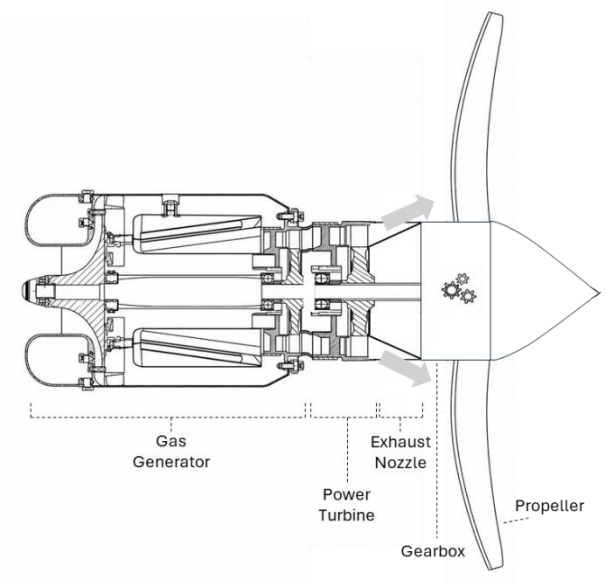


Figure 3 – Conceptual cross-section drawing of the MOJO engine with gearbox

To limit part count, mass and cost, the present study restricts the design to a single-stage power turbine. The maximum acceptable turbine loading for a single-stage turbine can be derived from literature. In this study, the stage loading coefficient $\Psi_{PT} = \frac{\Delta h_{PT}}{U_m{}^2}$ with $U_m = 2\pi \cdot n_{PT} \cdot R_{m,out}$ is limited to $\Psi_{PT} < 2$, according to [5]. Herein, Δh_{PT} is the enthalpy difference of the power turbine while U_m is the circumferential speed at the rotor outlet for the mean radius $R_{m,out}$ and for the rotational speed n_{PT}.

For a retrofittable solution, the power turbine diameter should be compatible with the gas generator geometry. As a first design approach, the hub diameter at the gas generator turbine exit is therefore kept equal to the hub diameter of the power turbine, avoiding a diameter change between both turbine sections.

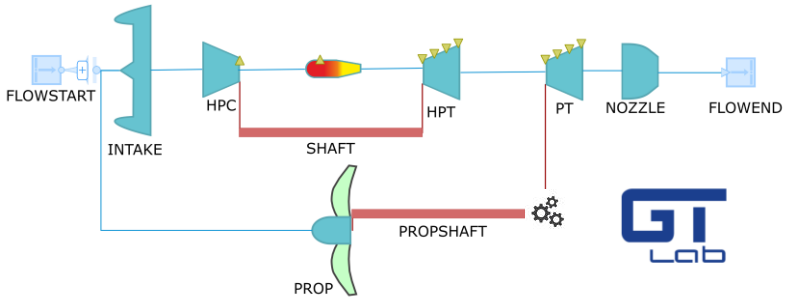


Figure 4 – MOJO performance model architecture with gearbox

Since the gearbox must be located in the hot section downstream of the turbine and close to the exhaust nozzle, implementing a fully axial nozzle becomes difficult. Such a configuration would require large ducting with drawbacks in weight and drag. In the present study, it is assumed that half of the theoretical nozzle thrust is lost due to non-axial nozzle flow. Consequently, the gross thrust coefficient of the nozzle is set to 50 %.

To avoid such losses, the nozzle pressure ratio is initially assumed to be 1.01 at the propeller design point. Despite the small pressure difference, the nozzle still contributes a certain fraction of the total thrust.

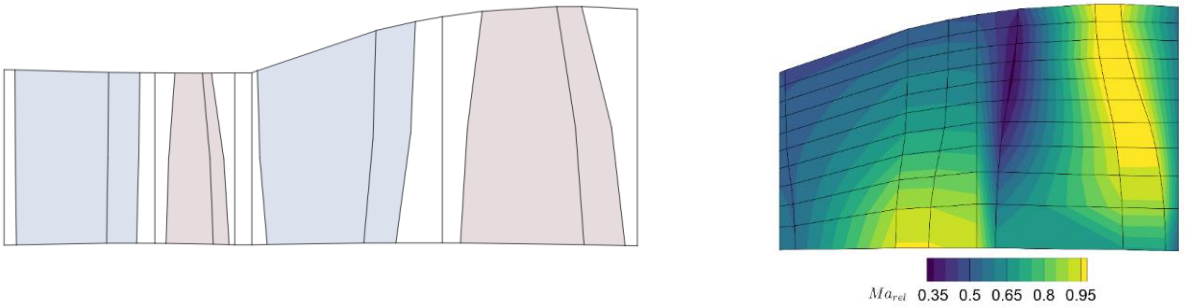
3.1 Turbine for geared MOJO configuration

The required circumferential speed of the single turbine stage can be calculated from the given cycle parameters and the selected stage loading. By estimating a representative Mach number upstream and downstream of the power turbine, the flow annulus can be derived by applying the continuity

equation at the turbine inlet and outlet. The resulting mean radius then allows the rotational speed to be determined from the circumferential speed. To estimate the turbine efficiency the efficiency correlation methodology from [6] was applied and resulted in an isentropic power turbine efficiency of 88 %.

Following the performance calculation, the 1D meanline program *PrEDiCT* ([7], [8], [9]) is used to generate an initial design of the power turbine based on a reduced set of requirements provided from the engine model, such as turbine power, shaft speed, mass flow, and inlet turbine flow conditions. With this information, *PrEDiCT* determines an annulus geometry and calculates the thermodynamic performance and losses for the turbine design. If desired, the initial turbine geometry can then be manually adjusted by the user until the performance and geometric requirements of the engine model are met. The turbine geometry for the geared MOJO configuration is shown in Figure 5a.

The circumferentially averaged flow field is calculated with the streamline curvature model *SLC4T* ([7], [8]) for the turbine design by extracting the turbine geometry along the S2m plane from *PrEDiCT*, as shown in Figure 5b. A turbine performance can subsequently be generated by calculating the flow field at various off-design points to further refine the engine level model.



(a) (b)

Figure 5 – (a): Turbine geometry generated from *PrEDiCT* for the HPT and geared power turbine (b): corresponding flow field of the power turbine showing the relative flow Mach number distribution

3.2 Propeller for the geared MOJO configuration

The propeller rotational speed is typically constrained by the blade-tip Mach number. For conventional propellers, transonic tip speeds are generally avoided because compressibility effects cause increasing efficiency losses. As an initial assumption, the propeller speed is therefore limited by a high subsonic tip Mach number of 0.95. In a typical turboprop engine design, aircraft integration considerations limit the maximum propeller diameter. In this study, such a limitation is not imposed.

Therefore, the baseline configuration uses a gear ratio of 6.5, which results in a propeller diameter of 0.84 m for the prescribed tip-Mach-number limit. Variations of the blade-tip Mach number, propeller diameter, and gear ratio are presented in Part II of this paper [10].

The gearbox itself is not designed in detail in the present study. Instead, it is represented by an assumed overall efficiency and by the required reduction ratio resulting from the selected turbine and propeller speeds. For the considered reduction ratio, a two-stage gearbox concept is assumed, since realizing the full reduction in a single planetary stage would be challenging with respect to gear sizing, load distribution, and efficiency. The overall gearbox efficiency is set to 99 %. Effects of gearbox mass, lubrication/cooling, and mechanical integration are not included in this performance assessment.

In this study, *PROPSTER*, DLR's in-house propeller conceptual design tool, is applied for the preliminary sizing of the propeller [11, 12]. *PROPSTER* is based on blade element theory and is used to estimate the aerodynamic performance of propeller configurations for different operating conditions. The tool provides performance quantities such as thrust, torque, shaft power, and propeller efficiency, and allows parametric variations of propeller diameter, rotational speed, blade number, and blade geometry.

The results from the conceptual propeller design are iteratively used within the performance model to provide a consistent propeller efficiency for the engine performance calculation. A sketch of the propeller is shown in Figure 6.

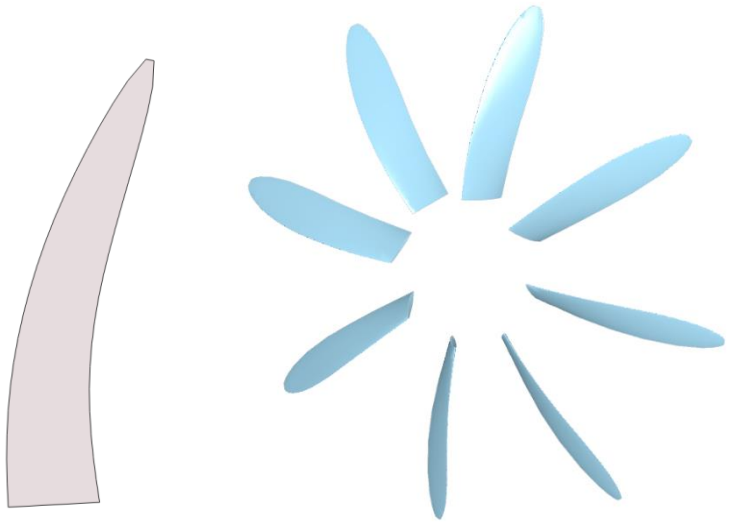


Figure 6 – Left: Initial propeller 2D blade projection from *PROPSTER*; Right: 3D view of the initial propeller design

4. Direct-drive MOJO configuration

Connecting a power turbine and a propeller without a gearbox is a highly challenging task and has not, to the authors' knowledge, been demonstrated for small turbojet-based propulsion systems. The most prominent large-scale example is the GE36 unducted fan, which employed a gearless contra-rotating arrangement in which two counter-rotating fan stages were driven by contra-rotating turbine stages [13].

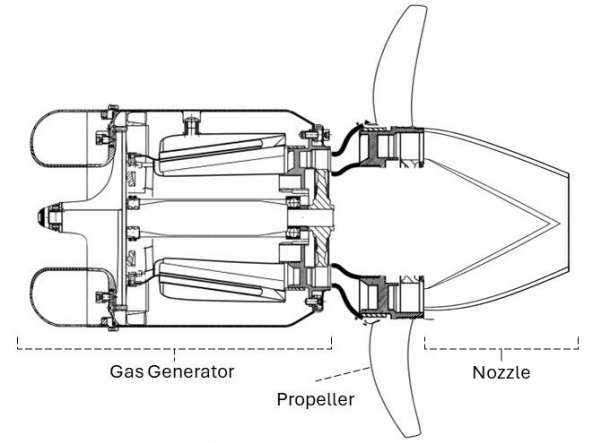


Figure 7 – Conceptual cross-section drawing of the direct-drive MOJO engine concept

Such a direct-drive architecture imposes significant compromises on both the turbine and the propeller, as both components must operate at a common rotational speed. For a retrofit application, however, a feasible direct-drive solution could offer a more compact, simpler rear-end architecture with fewer components and without a gearbox in the hot part of the engine.

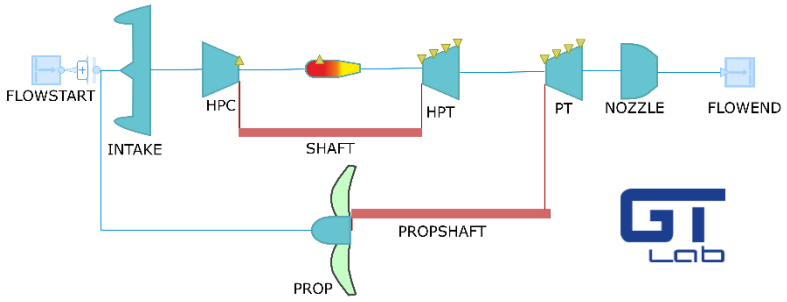


Figure 8 – MOJO performance model architecture for the direct-drive configuration

Directly attaching the propeller to the turbine rotor is demanding not only from an aerodynamic standpoint, but also with respect to thermal loading and material constraints. Conversely, this architecture may allow the conventional turbine disc to be eliminated by mounting the turbine blades on an outer rotating ring. This could improve the applicability of brittle but light materials such as ceramics.

The design approach for this configuration starts with the turbine, while accounting for the geometric constraints imposed by the gas generator and exploiting the available installation space. As an initial design assumption, the remaining nozzle pressure ratio at the design point is set to 1.29. This comparatively high value reduces the extractable power of the power turbine and thereby helps to limit the required rotational speed for a given maximum turbine stage loading. The sensitivity of the concept to this parameter, together with other design parameters, is investigated in Part II [10] of this paper.

A schematic concept illustration of the proposed configuration is shown in Figure 7. Again, the figure is intended to support the understanding of the overall engine architecture and component arrangement and should not be interpreted as a geometrically accurate representation of the calculated design.

4.1 Turbine design for direct-drive MOJO configuration

In order to allow direct coupling, the turbine must operate at a much lower rotational speed than in the geared configuration. To mitigate the resulting rotational speed mismatch between turbine and propeller, the available radial installation space is exploited by increasing the power turbine radius as far as permitted by the gas-generator geometry. It is assumed that the outer radius of the power turbine should not exceed the outer radius of the gas generator. Bridging the resulting radial offset between the gas generator and the power turbine therefore requires a long inter-turbine duct.

The stage loading of the turbine is further increased to avoid a second turbine stage while keeping rotational speed as low as possible. A challenging but nevertheless still feasible value of 2.5 is applied [5].

The applied efficiency correlation [6] found an initial isentropic turbine efficiency of 86 %. The same turbine conceptual design methodology as for the geared approach is applied. An initial sketch of such a turbine is shown in Figure 9 and its flow field in Figure 10.

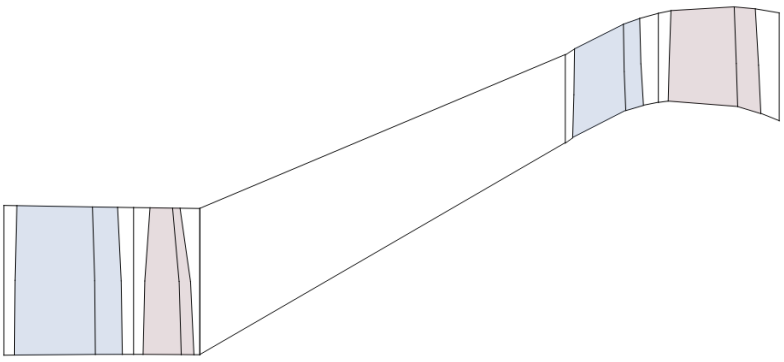


Figure 9 – Turbine geometry generated from *PrEDiCT* for the direct-drive turbine

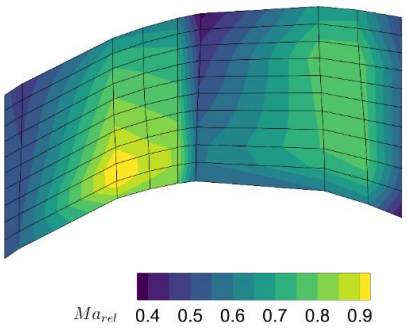


Figure 10 – Flow field in power turbine for the direct-drive turbine showing the relative flow Mach number distribution

4.2 Propeller design for direct-drive MOJO configuration

The turbine design described above, although already pushed towards low rotational speed, still requires a propeller rotational speed of approximately 18,000 rpm. Figure 11 shows the resulting propeller diameter as a function of the circumferential blade-tip Mach number. The results indicate that large propeller diameters are unsuitable for a direct-drive configuration. For example, the propeller from the geared concept would reach an unrealistic tip Mach number of 2. Even at comparatively small diameters, the circumferential blade-tip speed becomes transonic or supersonic.

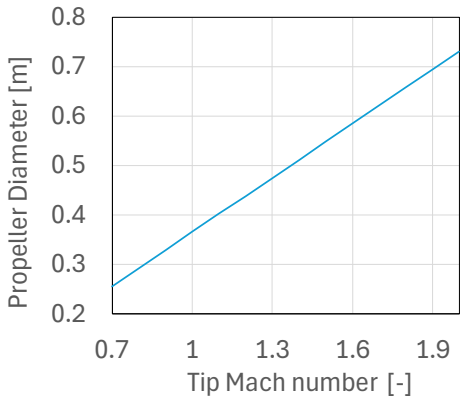


Figure 11 – Propeller diameter and tip Mach number

NACA tested full-scale turbine-driven supersonic propellers, and NASA Lewis later investigated swept high-speed propeller models operating at supersonic tip Mach numbers [14]. The present study focuses on the aerodynamic feasibility of such a propeller, keeping in mind that acoustic and mechanical challenges may pose serious constraints on its implementation.

For the direct-drive configuration, a blade-tip Mach number of 1.35 is selected, which results in a propeller diameter of 0.45 m. The sensitivity of the concept to the selected tip Mach number is investigated in Part II of this paper [10]. The propeller hub diameter is set equal to the outer diameter of the gas generator, leading to a hub-to-tip ratio of 0.52.

Due to the high blade-tip Mach numbers expected for this configuration, swept blades are assumed. The sweep angle distribution is based on NASA's SR-3 propeller [15] with a tip sweep of approximately 45°.

As for the geared configuration, *PROPSTER* is applied for the conceptual aerodynamic assessment of the propeller. As expected, the high blade-tip Mach number leads to a significant reduction in propeller efficiency. For the initial design, a propeller efficiency of 74 % is estimated. Figure 12 shows the resulting propeller geometry.

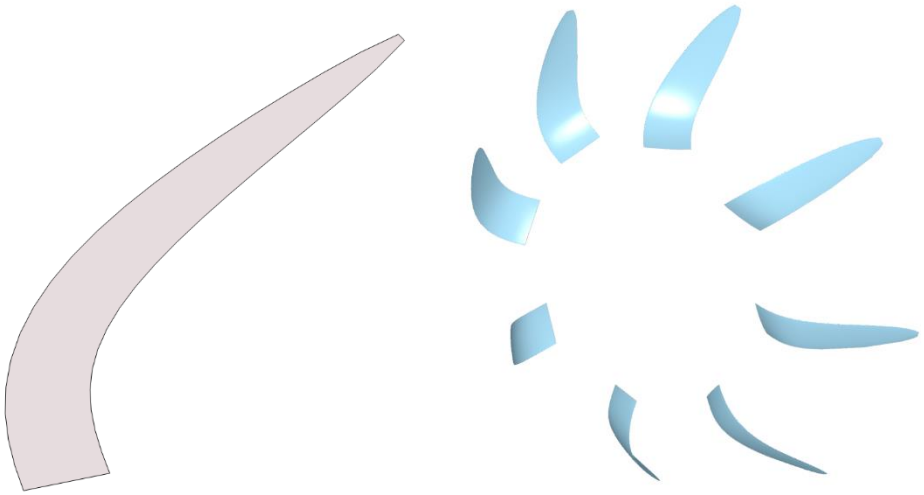


Figure 12 – Left: 2D projection of the propeller blade; Right: 3D view of the propeller design

Although the selected direct-drive propeller operates in a highly challenging regime, previous NASA high-speed propeller studies showed that thin, swept blades can mitigate compressibility losses at high relative Mach numbers [16]. The present design should therefore be interpreted as an aerodynamic concept study; its mechanical, aeroelastic and aeroacoustic feasibility remains open and may impose severe constraints on the achievable blade geometry and rotational speed.

5. Performance comparison

In Figure 13, the operating behavior of both MOJO configurations is shown for a given flight Mach number at sea level. For comparison, the corresponding behavior of the baseline gas generator as a jet engine is added for the same flight speed and for higher Mach numbers as well.

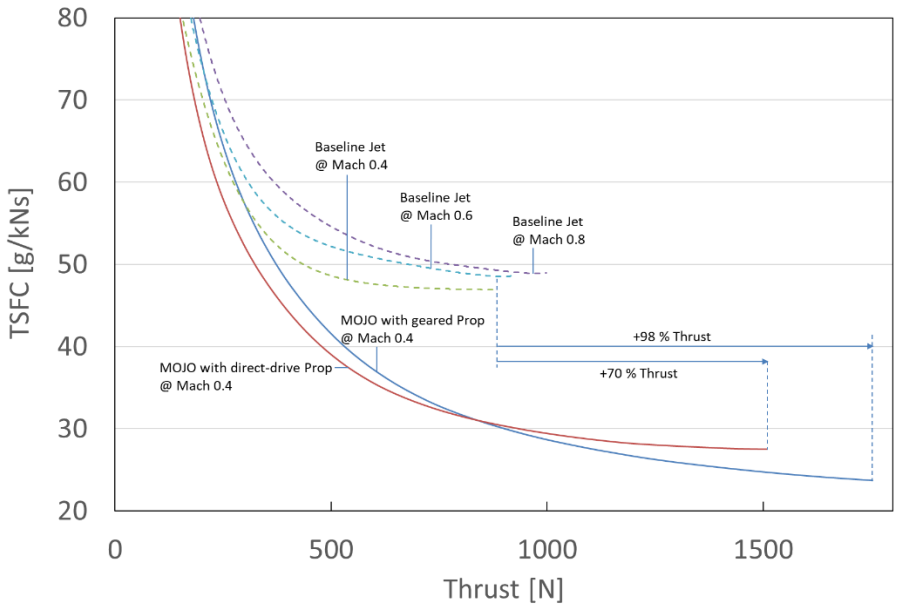


Figure 13 – Comparison of the thrust-specific fuel consumption and the available thrust at sea level

The propeller retrofit configurations show a substantially lower thrust-specific fuel consumption (TSFC) than the baseline gas generator operated as a jet engine. This reduction is mainly caused by the increased propulsive efficiency of the propeller. At the same full-load operating point, the fuel flow of the gas generator remains essentially unchanged; therefore, the improvement in TSFC results primarily from the large increase in thrust (+98 % for the geared propeller, +70 % for the direct-drive propeller) rather than from a reduction in fuel consumption.

The benefits of the propeller configurations are expected to decrease at higher flight speeds, where

the attainable propulsive-efficiency advantage becomes smaller. Depending on the intended application, this limitation may be acceptable, for example for military loiter missions or other operating points dominated by low-speed endurance.

Comparing the direct-drive and the geared MOJO design, the performance differences are substantially smaller than those observed between the baseline turbojet and the propeller-based retrofit configurations.

At high-thrust operating points, the direct-drive propeller configuration performs worse than the geared configuration. This difference is mainly caused by the lower propeller efficiency of the direct-drive concept. Since the propeller is directly coupled to the power turbine, its rotational speed is a compromise accounting for constraints from turbine design. Even though the turbine is already optimized for minimum rotational speed, the resulting propeller tip Mach number remains very high. This leads to increased losses and therefore to a lower propeller efficiency compared with the geared configuration, where the propeller speed can be selected independently.

The improved thrust production of the fully-axial exhaust nozzle of the direct-drive configuration is not sufficient to compensate for the loss in propeller efficiency and is further hindered by the low propulsive efficiency of the jet thrust due to the comparatively high remaining nozzle pressure ratio in the direct-drive configuration. At lower part load, the direct-drive MOJO design improves compared to the geared approach and is able to outperform it in terms of TSFC.

Overall, the geared configuration benefits from the ability to operate the propeller at a more favourable rotational speed and thus at higher propeller efficiency. The direct-drive configuration avoids the gearbox and can utilize a larger nozzle pressure ratio, but these advantages do not fully compensate for the aerodynamic penalties of the high-speed propeller and the lower propulsive efficiency of the jet contribution at high-thrust conditions.

The present comparison demonstrates the general potential and the main architectural limitations of the MOJO retrofit concept, but it remains based on selected initial design points. Since propeller diameter, rotational speed, tip Mach number, nozzle pressure ratio and power-turbine loading are strongly coupled, a broader design-space exploration is required to identify feasible design corridors and architecture-specific trade-offs. This is addressed in Part II of this paper, where the geared and direct-drive configurations are investigated using an integrated performance, propeller, turbine and mass-estimation process.

6. Conclusion and Outlook

The study demonstrates that a small turbojet engine can be used as a fixed gas generator and extended by a modular power-turbine/propeller unit without changing the gas generator. This indicates that a propeller-based retrofit can be evaluated as an add-on concept, in which the gas generator provides the required mass flow, pressure ratio, and turbine exit temperature for the downstream power turbine.

Compared with the baseline turbojet, both propeller-based retrofit configurations show the potential to substantially reduce thrust specific fuel consumption by increasing the effective propulsive efficiency of the overall engine.

The geared configuration provides the more robust performance solution, since the rotational speeds of the power turbine and the propeller can be selected independently. This allows both components to operate closer to their respective aerodynamic optima.

In contrast, the direct-drive configuration is attractive because it eliminates the gearbox, but its feasibility is constrained by the conflicting rotational-speed requirements of the turbine and propeller. The resulting high propeller tip Mach numbers lead to increased compressibility losses and reduced propeller efficiency. Under the assumptions applied in this study, the concept nevertheless appears aerodynamically feasible, although mechanical, aeroelastic, and aeroacoustic feasibility remain open.

The geared concept also provides substantially greater freedom in propeller design. These additional degrees of freedom are investigated in more detail in Part II and are expected to offer particular benefits for larger propeller diameters. Conversely, if the propeller diameter is severely constrained by the airframe or installation geometry, the relative performance penalty of the direct-drive concept may decrease, making its layout more attractive.

To further assess the potential of the direct-drive configuration, additional studies are required. These should address the mechanical feasibility of the propeller, the structural implementation of the propeller-turbine connection, and the aeroelastic implications of the resulting arrangement. Moreover,

the expected adverse aeroacoustic effects need to be analyzed, since they may limit the applicability of this configuration primarily to non-civil applications.

A more comprehensive component-level design-space exploration of both considered concepts, including detailed parameter sweeps of the power turbine and propeller for representative use cases, is presented separately in Part II.

7. Contact Author Email Address

Tom.Otten@dlr.de

8. Copyright Statement

The authors confirm that they, and/or their company or organization, hold copyright on all of the original material included in this paper. The authors also confirm that they have obtained permission, from the copyright holder of any third party material included in this paper, to publish it as part of their paper. The authors confirm that they give permission, or have obtained permission from the copyright holder of this paper, for the publication and distribution of this paper as part of the ICAS proceedings or as individual off-prints from the proceedings.

References

[1] Bradbrook S. J. *Common solutions to commercial and military propulsion requirements*, 24th International Congress of the Aeronautical Sciences, 2004.

[2] Sands J.S., Karl A.H., Mavris D.N. *Modelling and Simulation of Common Core Gas Turbine Engine Variant Applications*, Proceedings of ASME Turbo Expo 2016, GT2016-56394, Seoul, South Korea, 2016, https://doi.org/10.1115/GT2016-56394

[3] Schmidt R., Hupfer A. *Design and numerical simulation of ejector nozzles for very small turbojet engines*, CEAS Aeronautical Journal (2021) 12:923-940, https://doi.org/10.1007/s13272-021-00537-3

[4] Jetcat, Ingenieurbüro CAT, M. Zipperer GmbH, [Online]. Available: www.jetcat.de. [Accessed 15 05 2026].

[5] Grieb H., Projektierung von Turboflugtriebwerken., Springer-Verlag, 2013.

[6] Häßy J., Bolemant M., Becker R., "*An Educated Guess - Predicting Turbomachinery Efficiencies of Aero Engines During Conceptual Design*" Proceedings of ASME Turbo Expo 2023, GT2023-103638, Boston, Massachusetts, USA, 2023, https://doi.org/10.1115/GT2023-103638

[7] Krumme, K. *Performance Prediction and Early Design Code for Axial Turbines and its Application in Research and Predesign*, Proceedings of the ASME Turbo Expo 2016, GT2016-56082, Seoul, South Korea, 2016, https://doi.org/10.1115/GT2016-56082

[8] Grunwitz C., Nelles D., Carvalho F., Schöffler R., Brose N., Wehrel P. *A Comprehensive Multifidelity Design and Analysis Process for Cooled Axial Flow Turbines: From Concept to Component,* Proceedings of IGTC 2023, Kyoto, Japan, 2023, https://doi.org/10.58114/bdxv-4521

[9] Kost F. *Ein Verfahren zur Berechnung der Meridionalströmung von Axialturbinen*, DLR-Internal Report, DLR-IB 225-2014, 2014.

[10] Matuschek T., Otten T., Häßy J., Frank J., Brakmann R. Modular Jet and Propeller Engine - *Part II: Integrated Design Process and Design Space Assessment*, ICAS 2026, ICAS2026_0829, Sydney, Australia, 2026

[11] Häßy J. *Validierung und Implementierung eines Verfahrens zur Vorauslegung von Propellern auf Basis der Blattelementtheorie*, Bachelor Thesis, RWTH-Aachen, 2016

[12] Häßy J., *Untersuchung zum Einfluss des Propellers im Gesamtkontext der Triebwerksvorauslegung*, Master Thesis, RWTH Aachen, 2018

[13] GE Aircraft Engines, *Full Scale Technology Demonstration of a Modern Counterrotating Unducted Fan Engine Concept. Design Report*," NASA CR-180867, 1987

[14] Kurbjun M. C., *Noise Survey Under Static Conditions of a Turbine-Driven Full-Scale Modified Supersonic Propeller With an Advance Ratio of 3.2*, NACA-TN-4172, 1958

[15] Rohrbach C., Metzger F. B., Black D. M., Ladden R.M., *Evaluation of Wind Tunnel Performance Testings of an Advanced 45 Degree Swept Eight-Bladed Propeller at Mach Numbers from 0.45 to 0.85*, NASA CR-3505, 1982

[16] Jeracki R. J., Mikkelson D. C. and Blaha B. J. *Wind Tunnel Performance of Four Energy Efficient Propellers Designed for Mach 0.8 Cruise*. NASA Technical Memorandum 79124, Lewis Research Center, 1979.